

## INVESTIGATION OF FLOW AND TRANSPORT AT THE INTERFACE OF PERMEABLE SEDIMENTS IN THE VICINITY OF UPRISING BUBBLES USING LIF AND PIV

Michael Stöhr<sup>1</sup>, Afshin Goharzadeh<sup>1</sup>, Arzhang Khalili<sup>1, 2</sup>

<sup>1</sup>Max Planck Institute for Marine Microbiology, Celsiusstr. 1, 28359 Bremen, Germany

<sup>2</sup>International University Bremen, Campus Ring 1, 28759 Bremen, Germany

### Abstract

The transport of methane from marine sediments into the seawater and then into the atmosphere is important in the context of its role as a greenhouse gas. In the present work, we use an artificial laboratory setup in order to investigate the mechanisms of flow and transport induced by rising gas in a permeable sediment. A combination of the experimental techniques Particle Image Velocimetry (PIV), 3D Planar Laser-induced Fluorescence (3D PLIF) and refractive-index matching is employed for the visualization and quantification of different aspects of this multiphase flow phenomenon. We find that the gas, which is injected continuously into the sediment, forms a cone-shaped, vertical structure of trapped gas and leads to a spatially and temporally fluctuating escape of bubbles at the upper interface. The temporal variability of the total volume of trapped gas results in fluctuations of liquid velocities in the sediment pores and therefore leads to an enhanced mixing of solutes in the sediment. Furthermore, the highly resolved 3D PLIF data visualizes and quantifies the existence of a reverse, i.e. downward directed flow of liquid into the sediment induced by the rising gas. The presence of this downward flow in marine sediments may have important implications for the understanding and modeling of nutrient cycles and microbial life at the seafloor in the vicinity of methane seeps.

### Introduction

Methane is a long-living gas which receives considerable attention due to its role as a greenhouse gas in the atmosphere. Large amounts of methane are formed by microbial production in marine sediments, where it can escape to the surface and then into the atmosphere in the form of uprising bubbles (Leifer and Patro, 2002). The release into the atmosphere may be limited by microbial, anaerobic oxidation of methane (AOM) to CO<sub>2</sub> in anoxic sediments (Boetius et al., 2000). Since AOM requires oxidants like e.g. sulfate from the overlying seawater, the understanding of the transport of seawater solutes into the sediment is mandatory for a quantitative model of the fate of biogenic methane. While the efficiency of purely diffusive transport is rather low, the counter-current flow into the porous sediment induced by rising methane bubbles is a potentially much more efficient mechanism for the supply of oxidants from seawater into sediment. The knowledge about the shape and magnitude of this flow is, however, still vague.

The aim of the present study is the investigation of flow and transport in the vicinity of uprising bubbles near the interface of permeable sediments through laboratory experiments with artificial porous media. The two essential issues in this context are (1) the dynamics of gas inside the sediment and (2) the effect of the gas flow on the flow of vicinal liquid and thereby

on the transport of solutes. In order to accomplish an accurate optical 3D visualization, we employ the method of refractive index matching as described in (Stöhr et al., 2003). The measurement of flow and transport is attained by the techniques of particle image velocimetry (PIV) and 3D planar laser-induced fluorescence (3D PLIF).

### Experimental setup

The flow cell shown in figure 1 consists of a rectangular box with a square horizontal section area of  $96 \times 96 \text{ mm}^2$  and side-walls made of transparent Optiwhite™ glass with a height of 200 mm. It is filled up to the height of 60 mm with a homogeneous random packing of Duran glass beads with a diameter of  $d = 2.5 \text{ mm}$ . The porous matrix is saturated with a mixture of silicon oils (Dow Corning DC 550 and DC 556), and together with a 60 mm high layer of pure liquid on top of the matrix, the box is filled with silicon oils up to the height of 120 mm. In order to provide 3D optical access into the pore space, the mixing ratio of the silicone oils is tuned precisely so that the refractive indices of the oil mixture and the glass beads match accurately. Air is injected through a nozzle with an inner diameter of 2 mm mounted at the center of the container bottom. A tube connects the nozzle to a tubing pump where the desired flow rate can be applied.

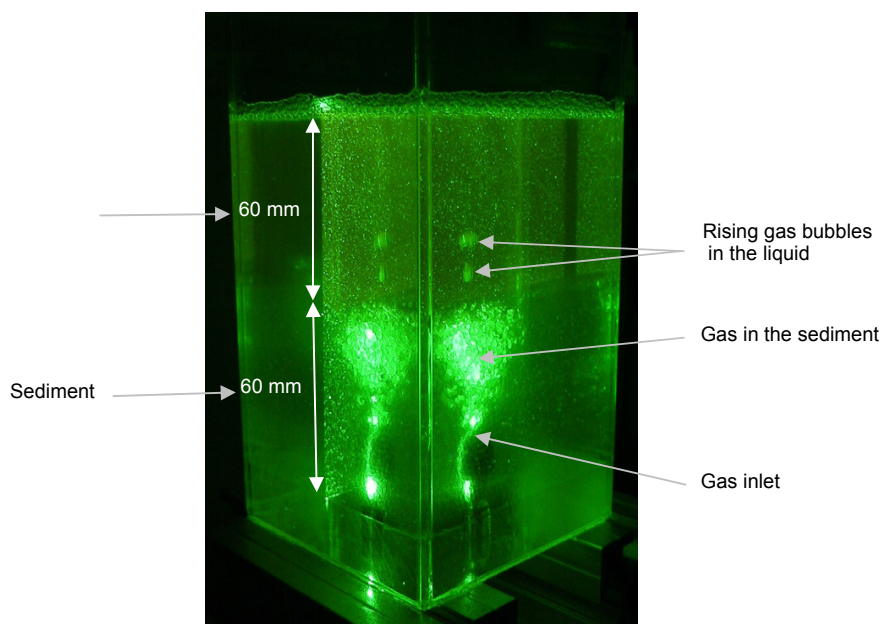


Figure 1: Photograph of flow cell illuminated with a laser light sheet for PIV and 3D PLIF measurements as sketched in figure 2.

The liquid velocities in both the porous layer and the liquid on top is examined by means of Particle Image Velocimetry. As shown in the figure 2, the laser pulses are produced by a pulsed YAG-laser ( $\lambda=532\text{nm}$ ) and transformed to a laser sheet using a cylindrical lens. The planar laser sheet penetrates the flow cell at a certain depth  $z$ . Polyamide particles with a diameter of  $5 \mu\text{m}$  were added to the fluid as tracer particles. A CCD camera (PCO Sensicam,  $1024 \times 1280$  pixels) was installed perpendicular to the plane of the laser sheet to record the particle motion in the field of view.

The method of PLIF is employed for investigating the transport of solutes in the liquid. A dissolved fluorescent dye (Nile Red) is excited by a planar laser sheet from a continuous-wave Nd-YAG laser (Laser Quantum Ventus, 532 nm, 1.5 W) with a wavelength suitable for the absorption band of the dye ( $\approx 500\text{-}600 \text{ nm}$ ). The light is re-emitted with an emission maxi-

mum at approx. 650 nm. The image of the 2D concentration distribution is then recorded by the CCD camera with an attached interference filter for the separation of the emitted light (see figure 2). In the present refractive index matched system the method can be extended to 3D by consecutively displacing both the camera and the laser sheet in the out-of-plane direction using a motorized translation stage. In the present setup, 100 images are taken during 20 s in the course of the displacement over 100 mm. Together with the reverse displacement and the storage of data to the harddisk, a 3D concentration distribution consisting of  $1024 \times 1280 \times 100$  12bit values is obtained every 40 seconds. These relative concentrations suffice for the present application, otherwise the measurement of absolute concentrations would be possible by performing a calibration with a solution of known concentration.

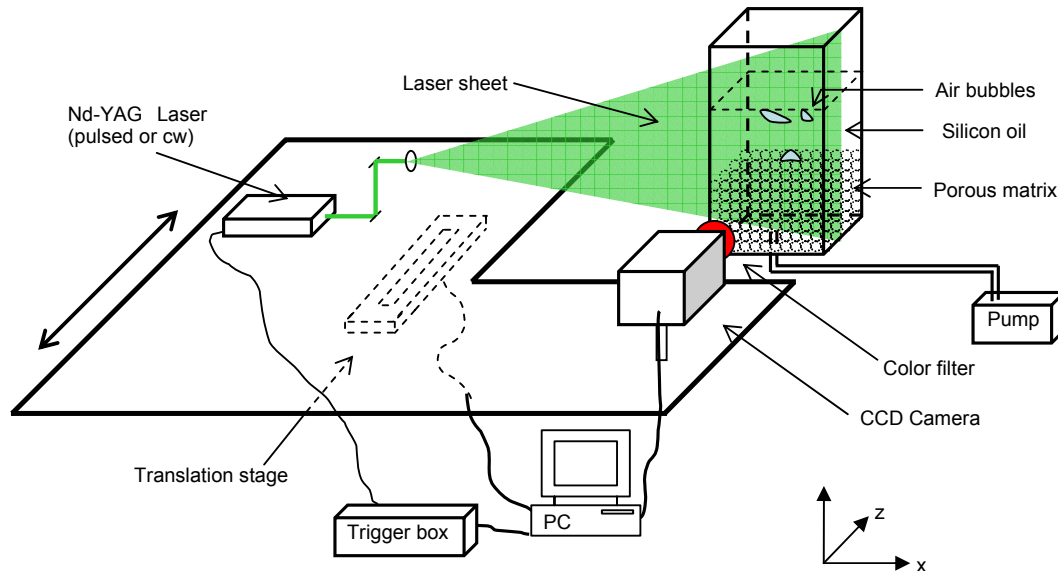


Figure 2: Sketch of experimental setup for 3D PLIF and PIV measurements.

Whereas the 3D visualization of flow and transport inside the saturated sediment could be accomplished by the matched refractive indices of solid and liquid as described above, this is obviously no longer possible for visualizing the distribution of gas in the sediment. To this end, the light scattering effect of gas bubbles is utilized for a 2D imaging of the gas as shown in figure 3. A 20 W halogen lamp illuminates a white paper at the backside of the medium, and the 2D projection of the gas distribution appears in the images of the CCD camera as dark regions on the white background from the paper (see figure 4). Images are taken with a reduced resolution of  $128 \times 320$  pixels, which allows for a higher frame rate (25 fps).

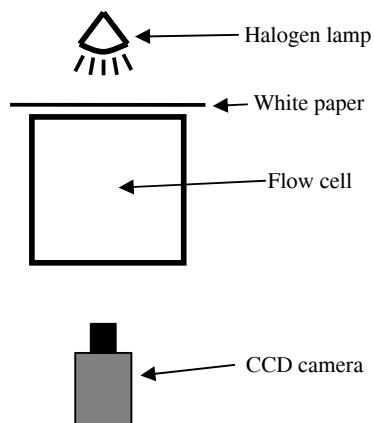


Figure 3: Sketch of the setup for the light transmission technique used for the visualization of gas inside the porous sediment.

## Dynamics of gas inside the sediment

The light transmission technique presented above has been employed for the visualization of gas in the sediment and liquid. After the preparation of a completely saturated sediment, air has been injected through the gas nozzle at the bottom with a constant flowrate of  $\approx 1$  l/h. The air escaped from the nozzle in the form of bubbles with diameters of few millimeters. The bubbles went upwards through the sediment along a large variety of individual paths, where they often became trapped. After about 10 min., the result is a cone-shaped area (upside-down with its tip at the nozzle) of trapped gas, which is shown in figure 4. This area stays then in a dynamic equilibrium, where trapped bubbles may become mobilized while mobile gas is trapped at other locations.

As shown in figure 4, the location where the bubbles escape from the sediment into the overlying liquid changes with time. These fluctuations behave intermittently, i.e. sometimes this location (and also the associated path of the rising bubbles) is static for several sec. or min., fluctuations can occur on all timescales and the systems never becomes completely stable. While air is injected continuously through the nozzle, the bubbles leave the sediment at discrete times. Consequently, the total volume of trapped gas fluctuates with the same time-scale as the escape of the bubbles. These fluctuations have implications for the flow inside the sediment, which will be discussed in the next section.

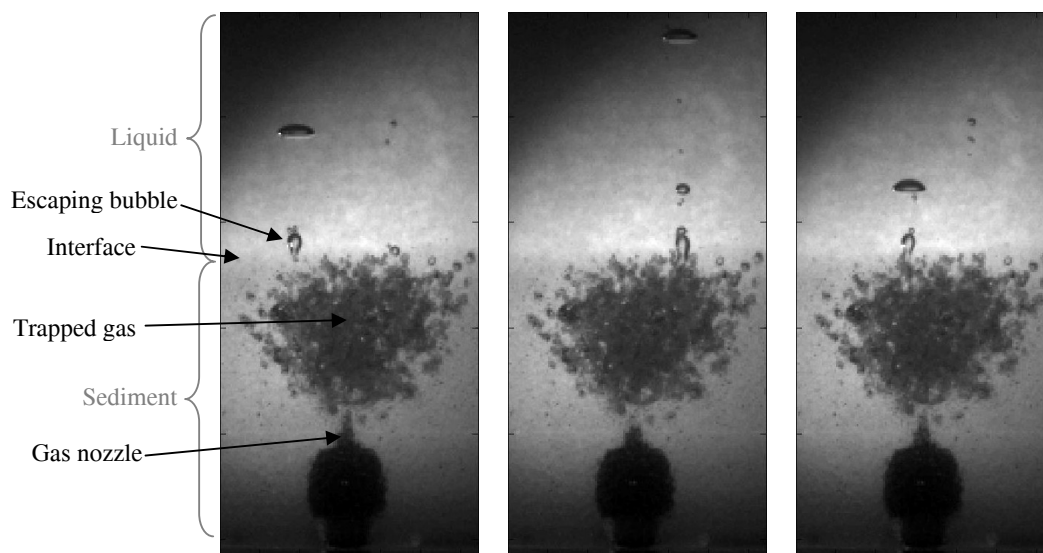


Figure 4: Spatial distribution of gas in the sediment and temporal dynamics of escaping bubbles at the sediment interface. Images are obtained with the light transmission technique described in section x. The images demonstrate the formation of a cone-shaped area of trapped gas in the sediment and the fluctuating locations of gas discharge at the interface.

## Liquid flow inside the sediment

The flow inside the porous matrix in a small field of view ( $16 \times 24$  mm<sup>2</sup>) was measured by PIV with a large separation time ( $\Delta t=100$ ms). The measurements focused on the fluid region between glass beads well below the permeable interface. Two examples of PIV images are shown in fig. 5 where the red hatched round areas show the locations of the glass beads. The beads have uniform diameter but may appear to be different in size because the laser sheet sections the spheres randomly and, hence, produces cross sections of different sizes. For the same reason, the beads seem to not always touch their neighbors. Fig. 5 represents instantaneous velocity field for two successive times (600 ms). In the figure 5a, the main direction of velocities is upwards and the in fig 5b, velocities are directed in downwards. This

rection of velocities is upwards and the in fig 5b, velocities are directed in downwards. This phenomenon is repeated irregularly for a long period.

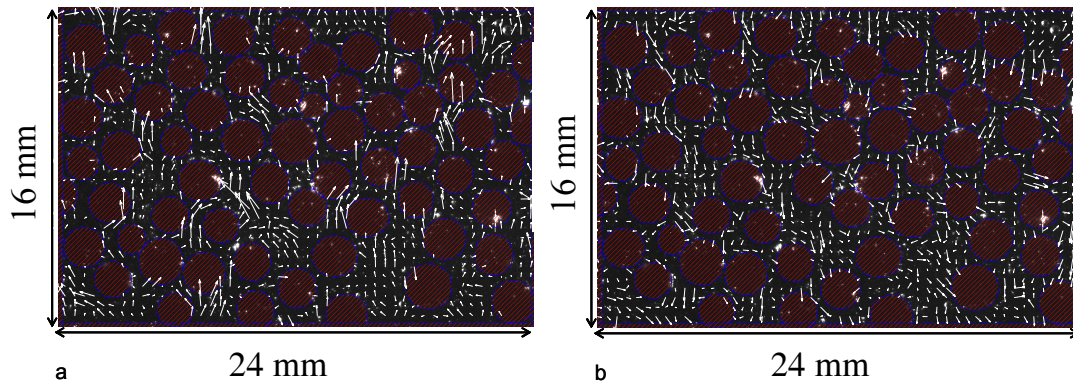


Figure 5: Fluctuations of instantaneous velocities inside the porous sediment characterized by alternating mean upward (a) and downward (b) flow.

Figure 6 shows the temporal evolution of vertical velocity, taken as a spatial average over the area shown in fig. 5. In the course of our investigation about the origin of these fluctuations, we have analyzed the data from the light transmission technique which was presented in the previous section. Here the bubbles are visualized by their shadow, and consequently the intensity of the image reflects the content of gas. As a rough estimate of the total gas content in the sediment, the mean image intensity in the sediment is plotted in fig. 6. Although these two time-series have not been recorded simultaneously, it is obvious that the series for vertical velocity and mean intensity have fluctuations on the same timescale. We therefore conclude that the fluctuations of the velocities in the sediment pores are caused by the dis- and replacement of liquid through the migrating and escaping gas in the center of the sediment: since the flow cell is open only at the top, the liquid can evade only in the vertical direction.

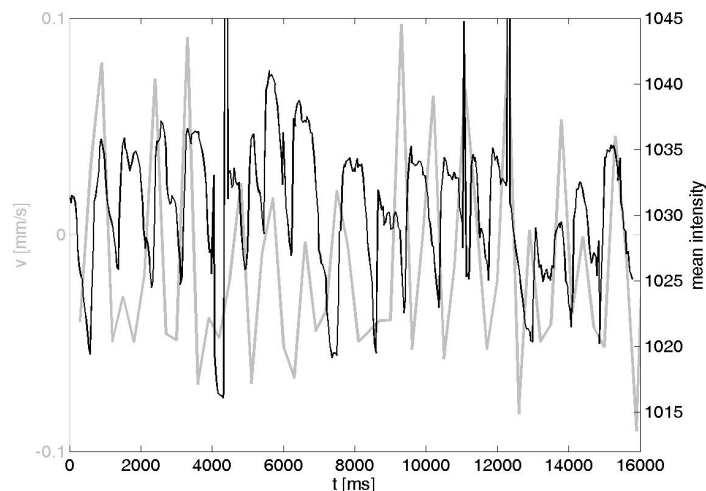


Figure 6: Comparison of fluctuations of vertical velocity in the sediment (gray) and mean transmitted light intensity (black) as a rough estimate of the total amount of gas in the sediment. The finding that both quantities fluctuate on a comparable timescale indicates that the velocity fluctuations are caused by the dis- and replacement of liquid by gas.

## **Solute transport from the liquid into the sediment**

The main goal of the present work, i.e. the analysis of the transport of solutes induced by rising gas, has been investigated using the 3D PLIF technique. At the beginning, the liquid above the sediment was homogeneously stained with the fluorescent dye, and then the air was injected with a flowrate of  $\approx 1$  l/h and a series of 180 3D concentration distributions has been recorded. The results shown in fig. 7 clearly indicate the downward transport of the dissolved dye from the liquid into the sediment. The downward velocities are rather constant in the x-y plane, with a small increase towards the center. From the 2D images in the left column, an average downward velocity of  $\approx 15$  mm/h can be estimated.

Obviously the dye is transported downwards also in the central cone-shaped region where the gas is rising upwards. This can be explained by the fluctuating paths of the rising gas in the sediment shown in figure 4: while the gas migrates upwards in a certain part of the cone-shaped area, the dye is transported downwards in the remaining part. In the temporal average, the dye invades the whole area.

Admittedly these results do not unambiguously prove that the downward transport of dye is caused by the uprising gas. In the above liquid the rising gas bubbles lead to a circulating flow structure with upward flow in the center and downflow near the walls. This flow potentially induces solute transport at the interface. In order to measure this effect, a vertical tube has been placed on the gas outlet so that the gas escapes directly at the interface into the liquid. Consequently the same circulating flow forms in the liquid, but no gas invades the sediment. The result of this experiment is shown in fig. 8 and demonstrates that the circulating flow indeed leads to a downward transport of dye. However, the magnitude of this effect is comparatively small with respect to the experiment with rising gas in the sediment.

## **Summary and conclusions**

In the present work, the phenomenological study of gas-liquid flow in a porous medium and its effect on solute transport at the interface has been accomplished using the techniques of refractive index matching, PIV and 3D PLIF. The following phenomena have been identified:

1. Gas injected into a homogeneous saturated porous medium consisting of  $d=2.5$ mm glass beads forms a cone-shaped area of trapped gas. The paths of rising gas bubbles and the locations of escaping bubbles at the top of the medium have an intermittently fluctuating temporal behavior.
2. The discontinuous discharge of individual bubbles from the sediment leads to the temporal variability of the total volume of gas trapped in the sediment. This results in fluctuations of liquid velocities in the sediment pores, whose magnitude ( $\approx 300$  mm/h) is significantly higher than the mean downward velocity ( $\approx 15$  mm/h). This effect leads to an enhanced mixing in the sediment.
3. The rising gas in the sediment induces a reversely directed flow from the overlying liquid into the sediment. Simultaneously the circulating flow in the liquid layer also leads to transport of solute at the interface. Its effect is, however, significantly smaller than that of the rising gas.

The results obtained in this study may have vital importance for the understanding and modeling of nutrient cycles and microbial life at the seafloor in the vicinity of methane seeps.

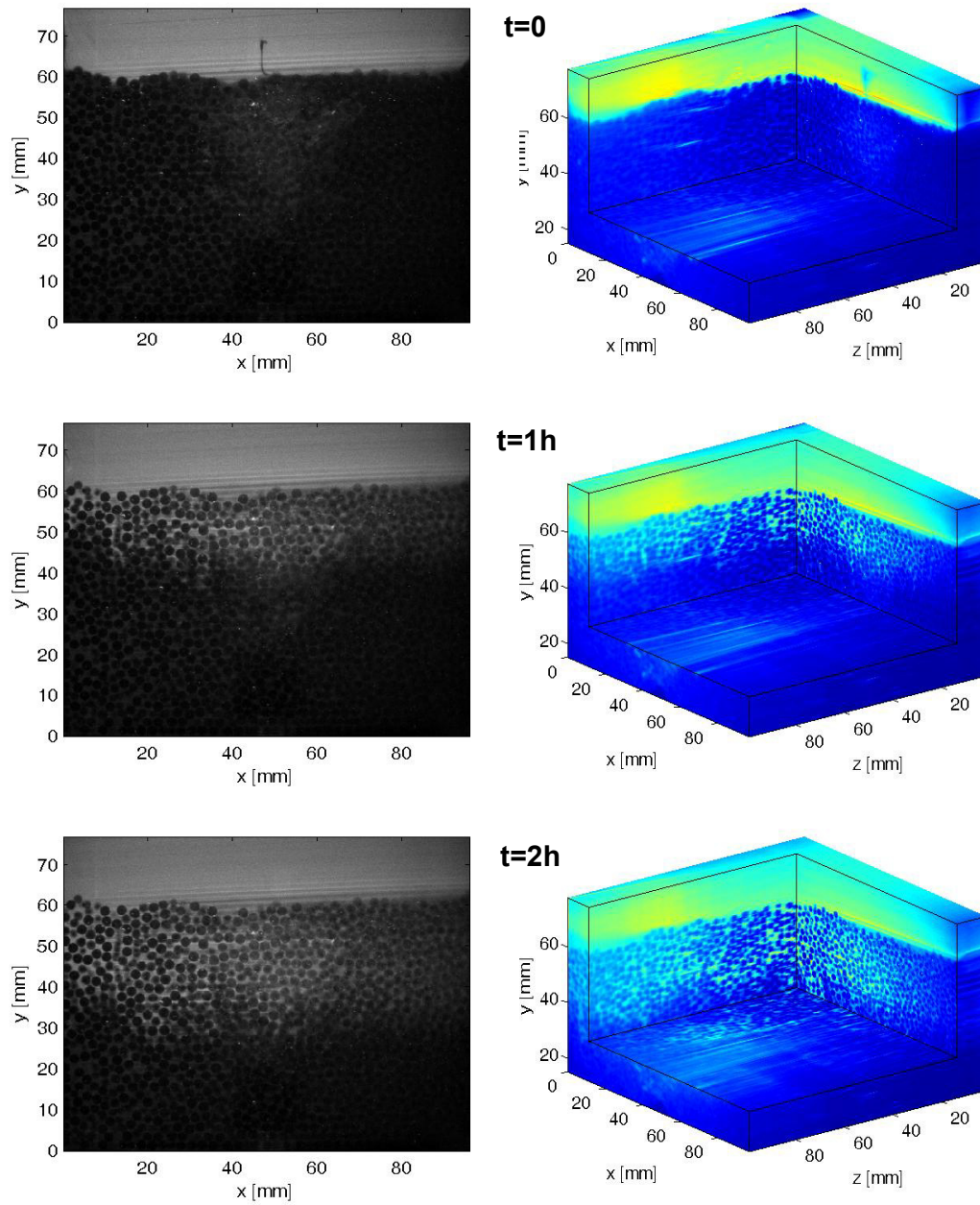


Figure 7: Temporal evolution of dye concentration in the flow cell during the upward gas flow in the center of the cell, shown at  $t=0$  (top),  $t=1\text{h}$  (middle) and  $t=2\text{h}$  (bottom). The left column shows the concentration in a  $96 \times 77 \text{ mm}^2$  plane at  $z=25\text{mm}$ , the right column the corresponding 3D volumes of  $96 \times 96 \times 62 \text{ mm}^3$ .

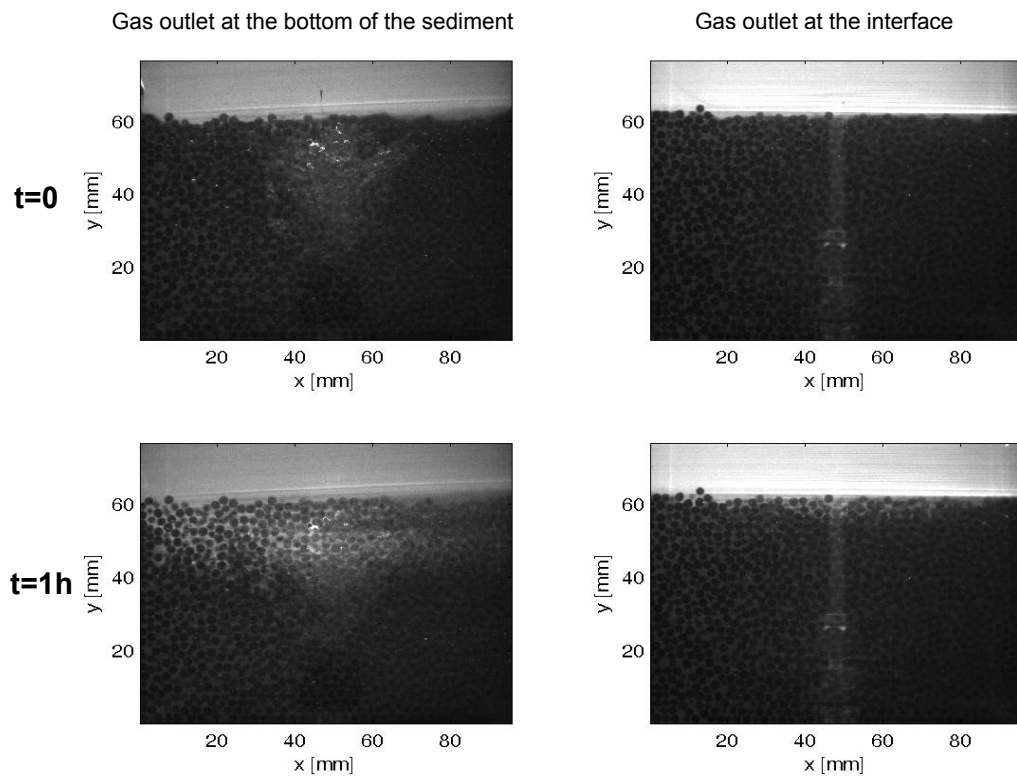


Figure 8: Comparison of solute transport induced by rising gas injected at the bottom of the sediment (left side) and gas injected at the interface (right side). The images demonstrate that the effect of the circulating liquid is small compared to the effect of the uprising gas in the sediment.

## Literatur

- Boetius, A., Ravensschlag, K., Schubert, C.J., Rickert, D., Widdel, F., Gieseke, A., Amann, R., Joergensen, B.B., Witte, U., Pfannkuche, O., 2000: A marine microbial consortium apparently mediating anaerobic oxidation of methane, *Nature*, 407, pp. 623-626
- Leifer, I., Patro, R.K., 2002: The bubble mechanism for methane transport from the shallow sea bed to the surface: A review and sensitivity study, *Continental Shelf Research*, 22, pp. 2409-2428.
- Stöhr, M., Roth, K., Jähne, B., 2003: Measurement of 3D pore-scale flow in index-matched porous media, *Exp. in Fluids*, 35, pp. 159-166